Modal Parameter Determination of Stay Cable with an Improved Algorithm Based on Stochastic Subspace Identification

Wen-Hwa Wu, Chien-Chou Chen, Shen-Wei Wang, Gwolong Lai

MODAL PARAMETER DETERMINATION OF STAY CABLE WITH AN IMPROVED ALGORITHM BASED ON STOCHASTIC SUBSPACE IDENTIFICATION

Wen-Hwa Wu [1], Chien-Chou Chen [1], Shen-Wei Wang [1], Gwolong Lai [1]

[1] *National Yunlin Unisersity of Science and Technology, No. 123, Sec. 3, University Rd., Touliu, Yunlin, 640 Taiwan*

wuwh@yuntech.edu.tw

ABSTRACT

The modal parameter determination of stay cable is generally a critical issue for either designing or monitoring cable-stayed bridges. Stochastic subspace identification (SSI) has been proved in recent years to be an excellent tool for obtaining all the modal parameters together in the cases where only the output signals are available. Nevertheless, its feasibility and accuracy in practical applications remain to be extensively verified. Especially for the situations where the frequency content of excitation is narrowly banded and thus far away from the white-noise assumption underneath the theoretical derivation of SSI, the problem of superfluously indentifying numerous deceptive modes usually occurs. Attempting to crack this difficulty, an improved algorithm based on SSI is developed in the current work for performing the modal parameter determination of stay cables. This study adopts the covariance type of SSI, usually with better stability and computation efficiency, to establish an effective methodology for extensively identifying the modal parameters of stay cables. Several details of choosing the computational parameters in performing SSI are first discussed, followed by proposing an alternative stabilization diagram such that most modal parameters of cable can stand out and then imposing appropriate sifting criteria to extract the most reliable modal parameters.

KEYWORDS : *modal parameter, stay cable, stochastic subspace identification, alternative stabilization diagram, sifting criterion.*

1 INSTRUCTION

An accurate estimation of stay cable forces typically play an important role in the health monitoring of cable-stayed bridges. Due to its simplicity, the conventional ambient vibration method is commonly adopted by first identifying the cable frequencies from the vibration measurements. With given vibration length and flexural rigidity, an analytical or empirical formula is then used with these cable frequencies to determine the cable force. It is, however, usually difficult to decide the vibration length due to the complicated boundary constraints at both anchorage ends. To tackle this problem, a novel concept of incorporating the mode shape ratios of cable was recently introduced by the authors to develop a convenient method for the determination of cable forces [1]. The success of this approach crucially depends on the effective identification of mode shape ratios based on multiple vibration signals simultaneously taken from the on-site measurement. Moreover, the stability problem of stay cables themselves due to the effect of wind is also a very important issue in design. In this case, the modal damping ratios of stay cables play a more significant role and need to be carefully investigated. Overall, the modal parameter determination of stay cable is generally a critical issue for either designing or monitoring cable-stayed bridges.

Stochastic subspace identification (SSI) has been proved in recent years to be an excellent tool for obtaining all the modal parameters together in the cases where only the output signals are available [2-3]. Consequently, the SSI technique is more and more popularly applied in the parameter identification of civil structures such as bridges and buildings. Nevertheless, its feasibility and accuracy in practical applications remain to be extensively verified. Especially for the situations where the frequency content of excitation is narrowly banded and thus far away from the white-noise assumption underneath the theoretical derivation of SSI, the problem of superfluously indentifying numerous deceptive modes usually occurs. Attempting to crack this difficulty, an improved algorithm based on SSI is developed in this work for performing the modal parameter determination of stay cables. The reason for choosing stay cable as the initial target to testify this new algorithm particularly resides in two aspects of its special dynamic characteristics. Unlike dealing with the irregular modal frequencies and widely spreading damping ratios for buildings or bridge decks, traditional techniques such as fast Fourier transform can be easily applied to obtain effective natural frequencies and mode shape ratios from the measurements on a stay cable because of its extremely light damping [4]. On the other hand, it has been pointed out in the literature that significant modal frequencies of the bridge girder can easily induce extra peak frequencies other than the cable frequencies in the Fourier amplitude spectra of cable measurements. From the cable's standpoint, these girder frequencies can be regarded as the particularly concentrated components in the frequency content of external excitation and may strongly interfere with the modal parameter identification of adjacent cable modes. Therefore, the modal parameter identification of stay cable concurrently provides a benchmark case with solid answers as well as a strict challenge for assessing the new SSI method.

2 COVARIANCE TYPE OF STOCHASTIC SUBSPACE IDENTIFICATION AND MODAL PARAMETERS

The numerical algorithms for SSI can be mainly classified into the covariance type and the data type. This study adopts the covariance type of SSI, usually with better stability and computation efficiency. Consider a structure system with n degrees of freedom (DOF) and its equations of motion under free vibration can be expressed as :

$$\mathbf{M}\ddot{\mathbf{w}}(t) + \Xi\dot{\mathbf{w}}(t) + \mathbf{K}\mathbf{w}(t) = \mathbf{0} \tag{1}$$

where $\mathbf{M}$, Ξ, and $\mathbf{K}$ represent the $n \times n$ mass matrix, damping matrix, stiffness matrix of structure, respectively. In addition, $\mathbf{w}(t)$ denotes the $n \times 1$ displacement vector for all the DOF's of structure. Definition of a $2n \times 1$ state vector to combine $\mathbf{w}(t)$ and $\dot{\mathbf{w}}(t)$ would further formulate Equation (1) in the state space as :

$$\dot{\mathbf{x}}(t) = \begin{bmatrix} \mathbf{0}_{n\times n} & \mathbf{I}_{n\times n} \\ -\mathbf{M}\Xi & -\mathbf{M}\mathbf{K} \end{bmatrix} \mathbf{x}(t) = \mathbf{A}_c \mathbf{x}(t) \tag{2}$$

where $\mathbf{A}_c$ is the $2n \times 2n$ system matrix. If output measurements are taken to obtain the $l \times 1$ output vector $\mathbf{y}(k)$ at the time instant $k\Delta t$, the whole set of state and output equations including the effect of noises can then be discretized with the sampling time increment Δt and arranged to:

$$\begin{cases} \mathbf{x}(k+1) = \mathbf{A}\mathbf{x}(k) + \mathbf{w}(k) \\ \mathbf{y}(k) = \mathbf{C}\mathbf{x}(k) + \mathbf{v}(k) \end{cases} \tag{3}$$

where $\mathbf{C}$ is the $l \times 2n$ output allocation matrix and $\mathbf{A} = e^{\mathbf{A}_c \Delta t}$ represents the discretized system matrix. Besides, $\mathbf{w}(k) \in R^{2n\times 1}$ and $\mathbf{v}(k) \in R^{l\times 1}$ signify the process noise vector and the measurement noise vector at the time instant $k\Delta t$, respectively. These two types of noises are usually difficult to be effectively assessed in practical applications and typically assumed in the SSI analysis as zero-mean white noises for the convenience in theoretical derivation.

The covariance matrix $\mathbf{H}_i \in R^{l \times l}$ for the output vector at a specified time lag $i\Delta t$ and the covariance matrix $\mathbf{G} \in R^{2n \times l}$ relating the output vector to the state vector can be defined as :

$$\mathbf{H}_i = \mathbf{y}(k+i)\mathbf{y}^{\mathrm{T}}(k); \;\; \mathbf{G} = \mathbf{x}(k+1)\mathbf{y}^{\mathrm{T}}(k) \tag{4}$$

With the assumption that both the two noise vectors are zero-mean white noises, it is straightforward to derive from Equation (3) that the two covariance matrices in Equation (4) are related by the system matrix **A** and the output allocation matrix **C** as [3]:

$$\mathbf{H}_i = \mathbf{C}\mathbf{A}^{i-1}\mathbf{G} \tag{5}$$

Systematic arrangement of the covariace matrices $\mathbf{H}_i$'s with different time lags would lead to a Teoplitz matrix:

$$\mathbf{T} = \begin{bmatrix} \mathbf{H}_i & \mathbf{H}_{i-1} & \cdots & \mathbf{H}_1 \\ \mathbf{H}_{i+1} & \mathbf{H}_i & \cdots & \mathbf{H}_2 \\ \vdots & \vdots & \ddots & \vdots \\ \mathbf{H}_{2i-1} & \mathbf{H}_{2i-2} & \cdots & \mathbf{H}_i \end{bmatrix}_{il \times il} \tag{6}$$

On the other hand, the output vectors $\mathbf{y}(k)$ measured at N consecutive time instants can also be organized into a Hankel matrix:

$$\mathbf{Y}_{0|2i-1} = \frac{1}{\sqrt{j}} \left[\begin{array}{cccc} \mathbf{y}(0) & \mathbf{y}(1) & \cdots & \mathbf{y}(j-1) \\ \mathbf{y}(1) & \mathbf{y}(2) & \cdots & \mathbf{y}(j) \\ \vdots & \vdots & \ddots & \vdots \\ \mathbf{y}(i-1) & \mathbf{y}(i) & \cdots & \mathbf{y}(i+j-2) \\ \hline \mathbf{y}(i) & \mathbf{y}(i+1) & \cdots & \mathbf{y}(i+j-1) \\ \mathbf{y}(i+1) & \mathbf{y}(i+2) & \cdots & \mathbf{y}(i+j) \\ \vdots & \vdots & \ddots & \vdots \\ \mathbf{y}(2i-1) & \mathbf{y}(2i) & \cdots & \mathbf{y}(2i+j-2) \end{array} \right]_{2il \times j} = \left[\begin{array}{c} \mathbf{Y}_{0|i-1} \\ \hline \mathbf{Y}_{i|2i-1} \end{array} \right] = \left[\begin{array}{c} \mathbf{Y}_p \\ \hline \mathbf{Y}_f \end{array} \right] \tag{7}$$

where $\mathbf{Y}_p \in R^{il \times j}$, $\mathbf{Y}_f \in R^{il \times j}$, and $j = N - 2i + 1$. Combination of Equations (4) to (7) yields

$$\begin{aligned} \mathbf{T} = \mathbf{Y}_p \mathbf{Y}_f^{\mathrm{T}} &= \begin{bmatrix} \mathbf{C}\mathbf{A}^{i-1}\mathbf{G} & \mathbf{C}\mathbf{A}^{i-2}\mathbf{G} & \cdots & \mathbf{C}\mathbf{G} \\ \mathbf{C}\mathbf{A}^{i}\mathbf{G} & \mathbf{C}\mathbf{A}^{i-1}\mathbf{G} & \cdots & \mathbf{C}\mathbf{A}\mathbf{G} \\ \vdots & \vdots & \ddots & \vdots \\ \mathbf{C}\mathbf{A}^{2i-2}\mathbf{G} & \mathbf{C}\mathbf{A}^{2i-3}\mathbf{G} & \cdots & \mathbf{C}\mathbf{A}^{i-1}\mathbf{G} \end{bmatrix} = \begin{bmatrix} \mathbf{C} \\ \mathbf{C}\mathbf{A} \\ \vdots \\ \mathbf{C}\mathbf{A}^{i-1} \end{bmatrix} \begin{bmatrix} \mathbf{A}^{i-1}\mathbf{G} & \mathbf{A}^{i-2}\mathbf{G} & \cdots & \mathbf{G} \end{bmatrix} \\ &= \mathbf{O}_i \mathbf{\Gamma}_i \end{aligned} \tag{8}$$

where $\mathbf{O}_i \in R^{il \times 2n}$ and $\mathbf{\Gamma}_i \in R^{2n \times il}$ are the so-called observability matrix and controllability matrix, respectively. Singular value decomposition (SVD) can then be conducted on $\mathbf{T} = \mathbf{Y}_p \mathbf{Y}_f^{\mathrm{T}}$ to obtain

$$\mathbf{T} = \mathbf{U}\mathbf{S}\mathbf{V}^{\mathrm{T}} = \begin{bmatrix} (\mathbf{U}_1)_{il \times 2n} & (\mathbf{U}_2)_{il \times n_1} \end{bmatrix} \begin{bmatrix} (\mathbf{S}_1)_{2n \times 2n} & \mathbf{0}_{2n \times n_1} \\ \mathbf{0}_{n_1 \times 2n} & (\mathbf{S}_2)_{n_1 \times n_1} \approx \mathbf{0}_{n_1 \times n_1} \end{bmatrix} \begin{bmatrix} (\mathbf{V}_1^{\mathrm{T}})_{2n \times il} \\ (\mathbf{V}_2^{\mathrm{T}})_{n_1 \times il} \end{bmatrix} \approx \mathbf{U}_1 \mathbf{S}_1 \mathbf{V}_1^{\mathrm{T}} \tag{9}$$

where $n_1 = il - 2n$, **U** and **V** are orthogonal matrices, and **S** is a quasi-diagonal matrix with positive diagonal elements arranged in a decreasing order. Comparison of Equations (8) and (9) gives

$$\mathbf{O}_i = \mathbf{U}_1\mathbf{S}_1^{1/2}; \quad \mathbf{\Gamma}_i = \mathbf{S}_1^{1/2}\mathbf{V}_1^{\mathrm{T}} \tag{10}$$

If $\mathbf{O}_i$ is re-formulate from Equation (8) as :

$$\mathbf{O}_i\left((l+1):li,:\right) = \begin{bmatrix} \mathbf{CA} \\ \mathbf{CA}^2 \\ \vdots \\ \mathbf{CA}^{i-1} \end{bmatrix} = \begin{bmatrix} \mathbf{C} \\ \mathbf{CA} \\ \vdots \\ \mathbf{CA}^{i-2} \end{bmatrix} \mathbf{A} = \mathbf{O}_i\left(1:l(i-1),:\right)\mathbf{A} \tag{11}$$

then the discretized system matrix **A** can be determined by

$$\mathbf{A} = \mathbf{O}_i^{\oplus}\left(1:l(i-1),:\right)\mathbf{O}_i\left((l+1):li,:\right) \tag{12}$$

where the symbol $\oplus$ means to take the pseudo inverse.

With the obtained **A**, its eigenvalues $\tilde{\lambda}_k$'s are subsequently solved to further acquire the eigenvalues λ_k 's of the system matrix $\mathbf{A}_c$ based on the following relationship:

$$\tilde{\lambda}_k = e^{\lambda_k \Delta t}, \quad k = 1, 2, \cdots\cdots, 2n \tag{13}$$

According to the theory of linear systems, the modal frequencies ω_k 's and damping ratios ξ_k 's of structure can readily be calculated from λ_k 's which theoretically appear in complex-conjugate pairs and hold the following relationship:

$$\lambda_{2k-1}, \lambda_{2k} = -\xi_k\omega_k \pm \mathrm{i}\omega_k\sqrt{1-\xi_k^2}, \quad k = 1, 2, \cdots\cdots, n \tag{14}$$

Moreover, the eigenvectors of $\mathbf{A}_c$ are the same as those of **A** and also in complex-conjugate pairs according to the matrix theory:

$$\boldsymbol{\phi}_{2k-1} = \overline{\boldsymbol{\phi}}_{2k}, \quad k = 1, 2, \cdots\cdots, n \tag{15}$$

Since the latter part of Equation (11) implies that the output allocation matrix can be decided from

$$\mathbf{C} = \mathbf{O}_i\left(1:l,:\right) \tag{16}$$

it is then utilized to obtain the mode shape ratios at the output measurement locations by

$$\boldsymbol{\varphi}_k = \mathbf{C}\boldsymbol{\phi}_{2k-1} = \mathbf{O}_i\left(1:l,:\right)\boldsymbol{\phi}_{2k-1} \quad \text{or} \quad \boldsymbol{\varphi}_k = \mathbf{C}\boldsymbol{\phi}_{2k} = \mathbf{O}_i\left(1:l,:\right)\boldsymbol{\phi}_{2k}, \quad k = 1, 2, \cdots\cdots, n \tag{17}$$

Even though $\boldsymbol{\varphi}_k$ computed with Equation (17) is generally a complex-valued vector, further normalization with respect to any of its reference element should result in a vector with minor imaginary parts in all the elements because the mode shape ratios are theoretically real. This fact can consequently be exploited to check the effectiveness of these mode shape ratios.

3 CONVENTIONAL STABILIZATION DIAGRAM

The ambient vibration measurement for the longest stay cable R33 of Chi-Lu Bridge is first taken as an example in this study to demonstrate the difficulties in attemping the identification of parameters for numerous modes by applying the SSI techniques. The design length of this cable is 118.2m and the in-plane vertical component of cable vibration was recorded by high resolution velocimeters VSE-15D made by Tokyo Sokushin. The measurement duration was set at 300 sec with a sampling rate of 200 Hz. Aimed to also estimate the mode shape ratios of Cable R33, 4 velocimeters were installed at different positions on this cable to record the synchronized vibration signals. For the convenience in practical operations, all these 4 sensor locations were selected to be close to the bridge deck and their distances to the front end of the bottom rubber constraint are 1.5 m, .3.5 m, 5.5 m, and 7.5 m, respectively.

The conventional approach to determine the modal parameters with the SSI analysis generally needs to designate the time lag $i\Delta t$ first and then vary the selection of system order n. The identified results for different choices of n are typically plotted in the so-called stabilization diagram to observe the stability of modal parameters with the increasing value of n. It is noteworthy from Equation (9) that $il - 2n = n_1 \geq 0$ or $n \leq il/2$, i.e., the upper limit of the selected system order n is controlled by the time lag parameter i. For the applications in the parameter identification of bridge decks or buildings, it is often the case that only a few modes are required to effectively describe the dynamic behavior of structure. Accordingly, the selection of a very high value for the time lag parameter i in these cases is not necessary, usually a value under $i = 100$ or even $i = 50$ is more than sufficient. This rule of thumb, however, is severely challanged in the case of stay cables where a number of modes can noticeably contribute to their ambient vibration signals. The SSI analysis conducted with the measurements of Cable R33 is presented herein to illustrate such a problem. The conventional stabilization diagrams corresponding to $i = 100$ and $i = 300$ are displayed in Figures 1(a) and 1(b), respectively. For the case of $i = 100$, the stabilization diagram in the frequency interval from 0 to 10Hz barely shows a couple of stable modal frequencies and this performance is far worse than examing the corresponding Fourier amplitude spectra (FAS) as shown in the background of this figure. A note should be made that the modal frequencies of a long stay cable basically follow an arithmatic sequence according to the string theory. This equally spaced distribution of frequencies together with the characteristic of extremely light damping render the possible identification of quite a few modal frequencies simply by FAS. Even if the time lag is raised up to $i = 300$, Figure 1(b) indicates that most of the cable frequencies in this frequency range can be obtained from the stabilization diagram, but another problem of superfluously indentifying numerous deceptive modes may also occur.

4 ALTERNATIVE STABILIZATION DIAGRAM AND SIFTING CRITERIA

Primarily based on the consideration of computation efficiency, the conventional SSI analysis first choose the time lag parameter i and then alter the system order n to plot the stabilization diagram for discriminate the stable modes of structure. This approach encounters a great difficulty in the analysis for stay cables, as revealed in the previous section. This study proposes an alternative way to construct the stabilization diagram by fixing the system order n first and then varying the time lag

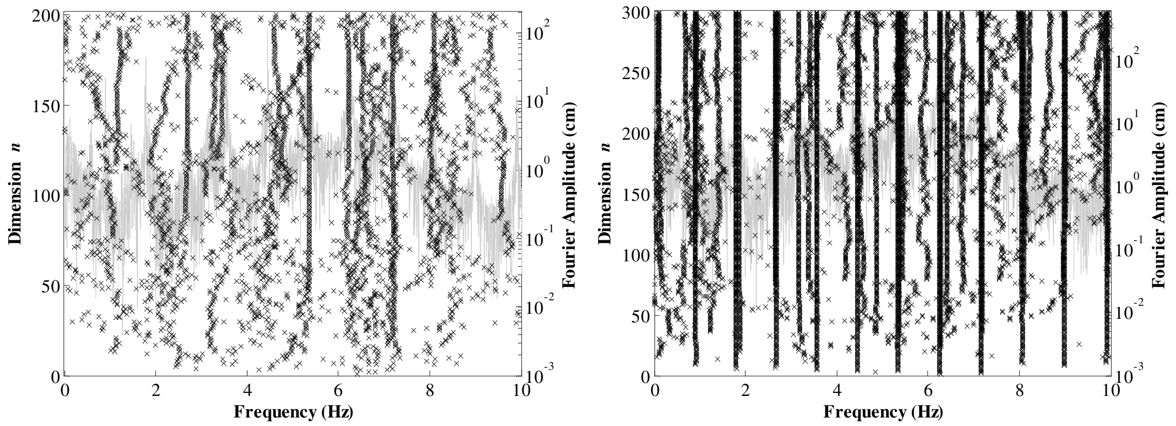

(a) i =100 (b) i =300

Figure 1: Conventional stabilization diagrams for SSI analysis of Cable R33 with different time lags

parameter i. Such a change is mainly inspired by the concept that the major contributed modes obtained from the SSI analysis should reach a stable level as long as the designated value of n is sufficiently large to adequately represent the structure system. With the same ambient vibration measurement for Cable R33, the system order is fixed at $n = 100$ and the time lag parameter is increased from $i = 50$ to perform the SSI analysis and establish the alternative stabilization diagram as shown in Figure 2. Comparison of Figures 1 and 2 elucidates that the alternative stabilization diagram holds the advantage in less interference from the superfluous modes.

Even with the alternative stabilization diagram to provide a better foundation for more effective identification of cable modes, the task of extracting reliable modal parameters from this diagram requires much more efforts. An automatic algorithm is first suggested in this work to carry out the preliminary sifting process such that close frequency values would be assigned to each appropriate group they are supposed to fit in. A pre-determined length of frequency segment is applied to divide any frequency interval of interest into numerous subintervals. In this case, the length of 0.1 Hz is adopted to divide the interval from 0 to 10 Hz into 100 subintervals. Each frequency value appearing in the stabilization diagram is then classified into its corresponding subinterval. The number of frequency values collected in each subinterval is directly related to its possibility of being a valid mode. Depending on the varying range of the time lag parameter i, a threshold number can subsequently be set to determine the qualified subintervals and also filter out all the frequency values in the other subintervals. For the results of Figure 2, the threshold number is set at 200 to obtain 14 qualified subintervals as depicted in Figure 3.

Following the preliminary sifting process described above, three stages of refining procedures are designed in this study to guarantee the quality of remaining modal parameters. The first stage is to sort more than 200 modal frequency values in each qualified subinterval and select the 100 consecutive frequency values with the smallest span. This smallest span is further required to be no larger than 0.01 Hz for its group to survive the first round of purification. As illustrated in Figure 4, there are totally 12 groups left after this round of operation. It is not difficult to observe from this figure that 11 of these 12 groups correspond to the cable frequencies due to their equally-spaced separation in the frequency domain. The only group that doest not fall into the above category is possibly induced by the frequency of bridge deck. For each group surving from the first stage, all damping ratios corresponding to its 100 frequency values are investigated in the second stage. Again, these 100 damping ratios are sorted to pick the 50 consecutive damping values with the smallest span. Figure 5 displays this stage of refining with red circles to represent the 50 selected damping values in each surviving group. It can be observed that the damping ratios are generally far more dispersed than their corresponding frequency values. After the purification of this stage, a few modes (4th, 5th, 7th, and 8th) exhibit particularly concentrated damping values, while the other modes may hold a much larger span at a still acceptable order of 0.1%. It should be especially emphasized that one group from Figure 4 is excluded in Figure 5 because of its much wider range

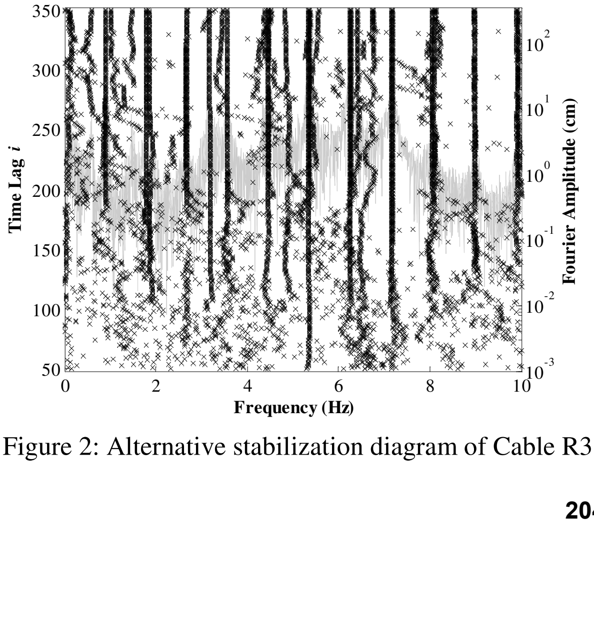

Figure 2: Alternative stabilization diagram of Cable R33

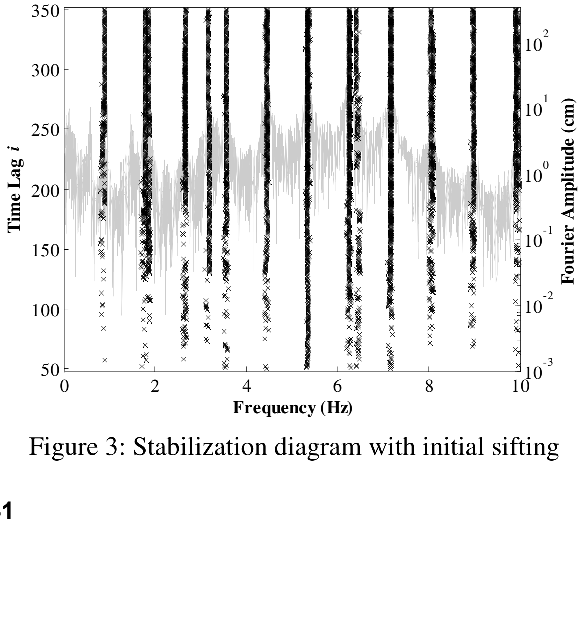

Figure 3: Stabilization diagram with initial sifting

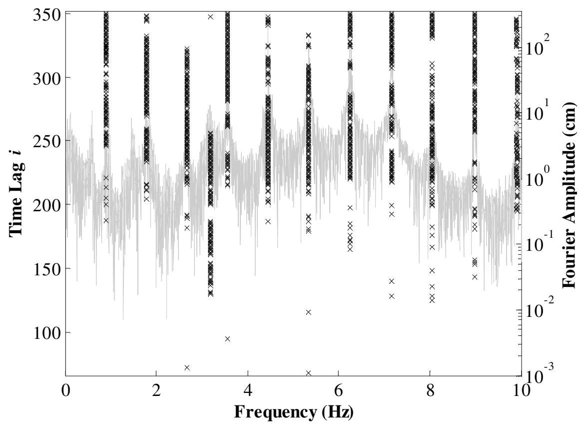

Figure 4: Stabilization diagram with 1st stage refining

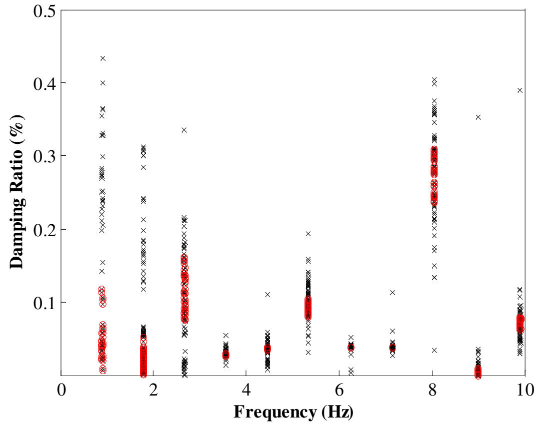

Figure 5: Damping diagram with 2nd stage refining

and exceptionally large values of damping ratio. Engineering judgement can be easily made to tell that this does not belong to a cable mode.

The 50 frequency values and their corresponding damping ratios of each mode surviving the second stage finally go to the third stage for examining the consistency of their corresponding mode shape ratios. A consistency index is defined as

$$\alpha_{ij} = \left|\boldsymbol{\varphi}_i - \boldsymbol{\varphi}_j\right| = \sqrt{\sum_{k=1}^{l}\left(\varphi_{ik} - \varphi_{jk}\right)^2},\ \ i,\ j = 1, 2, \cdots\cdots, 50 \tag{18}$$

in this study to do the job. In Equation (18), each normalized vector of mode shape ratios $\boldsymbol{\varphi}_i$ is composed by its components φ_{ik}'s and of unit length. A zero value of α_{ij} indicates a perfect

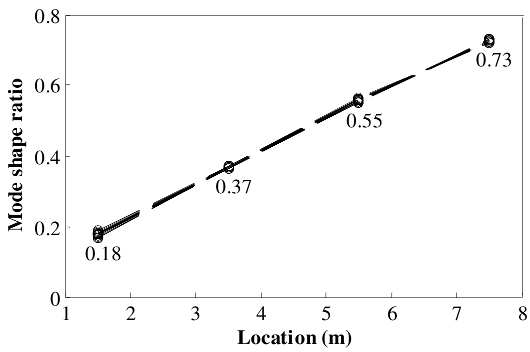

(a) 1st mode

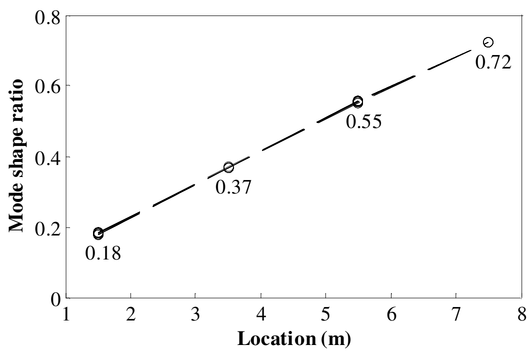

(b) 2nd mode

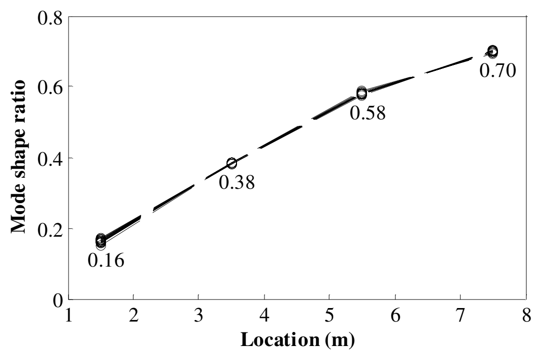

(c) 3rd mode

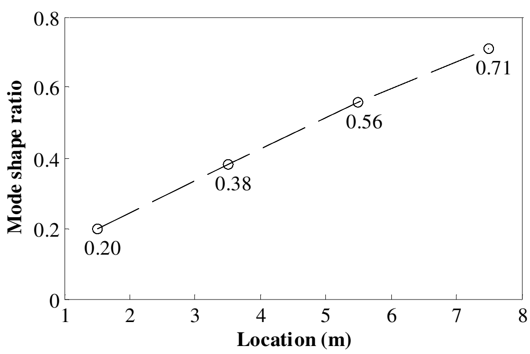

(d) 4th mode

Figure 6: Diagram of mode shape ratios with 3rd stage refining

Table 1: Modal parameters of Cable R33

Mode	Modal Frequency (Hz)	Damping Ratio (%)	Mode Shape Ratios at (1.5m, 3.5m, 5.5m, 7.5m)
1st	0.90	0.03	(0.18, 0.37, 0.55, 0.73)
2nd	1.78	0.02	(0.18, 0.37, 0.55, 0.72)
3rd	2.67	0.11	(0.16, 0.38, 0.58, 0.70)
4th	3.56	0.03	(0.20, 0.38, 0.56, 0.71)
5th	4.45	0.04	(0.21, 0.39, 0.56, 0.70)
6th	5.34	0.09	(0.23, 0.42, 0.58, 0.66)
7th	6.25	0.04	(0.23, 0.43, 0.58, 0.65)
8th	7.16	0.04	(0.25, 0.45, 0.59, 0.62)
9th	8.05	0.28	(0.31, 0.50, 0.60, 0.55)
10th	8.99	0.00	(0.28, 0.52, 0.61, 0.53)
11th	9.91	0.07	(0.33, 0.56, 0.61, 0.46)

consistency, while the larger value for this index implies more inconsistency. A 50×50 symmetric matrix with all zero diagonal elements can be established from Equation (18) for the 50 sets of mode shape ratios belongs to each mode. The average of the 49 elements other than the diagonal one for each column (or raw) can be considered as an average distance of any vector of mode shape ratios to the other 49 ones. A threshold of 0.02 is adopted in this work to filter out any set of mode shape ratios with a larger average distance than it. Figure 6 portrays this stage of refining for the first 4 modes. In fact, it is found that at most one out of 50 sets of mode shape ratios is excluded at this final stage of refining for all the 11 modes within the frequency interval of interest.

After going through all the three stages of refining, the remained frequency values, damping ratios, and mode shape ratios for each mode are averaged to obtain its corresponding modal parameters. All the results for the first 11 modes of Cable R33 are listed in Table 1.

5 CONCLUSIONS

This study adopts the covariance type of SSI, usually with better stability and computation efficiency, to establish an effective methodology for extensively identifying the modal parameters of a stay cable. Several details of choosing the computational parameters in performing SSI are first discussed, followed by proposing an alternative stabilization diagram such that most modal parameters of cable can stand out and then imposing appropriate sifting criteria to extract the most reliable modal parameters. Demonstrated by analyzing the ambient vibration measurements for the longest stay cable of Chi-Lu Bridge located in central Taiwan, the feasibility of the developed new methodology is further verified with successfully obtaining the modal frequencies, damping ratios, and mode shape ratios for the first 11 modes.

REFERENCES

[1] C.-C. Chen, W.-H. Wu, C.-H. Huang, G.-L. Lai. Determination of Stay Cable Force Based on Effective Vibration Length Accurately Estimated from Multiple Measurements. *Smart Structures and Systems*. 11:411-433, 2013.

[2] P. Van Overschee, B. De Moore. *Subspace Identification for Linear Systems: Theory-Implementation-Applications*. Kluwer Academic Publishers, 1996.

[3] B. Peeters, G. De Roeck. Reference-Based Stochastic Subspace Identification for Output-Only Modal Analysis. *Mechanical Systems and Signal Processing*. 13:855-878, 1999.

[4] W.-H. Wu, C.-C. Chen, J.-A. Liau. A Multiple Random Decrement Method for Modal Parameter Identification of Stay Cables Based on Ambient Vibration Signals. *Advances in Structural Engineering*. 15:969-982, 2012.